ISSN 1063-455X, Journal of Water Chemistry and Technology, 2019, Vol. 41, No. 3, pp. 175–181. © Allerton Press, Inc., 2019.

ANALYTICAL WATER CHEMISTRY

"Chitosan/Montmorillonite" Nanocomposites: Adsorption of Cr(III)[1]

Nadia Eladlani[a, b, *], El Montassir Dahmane[b], El-houssaine Ablouh[a, b], Abdelaaziz Ouahrouch[b], Mohammed Rhazi[a], Moha Taourirte[b], and Mounsef Neffa[b, c]

[a]*Équipe des Macromolécules Naturelles, Departement of Chemistry-Biologie,*
Ecole Normale Supérieure, University Cadi Ayyad Marrakech, Marrakech, Morocco
[b]*Laboratoire de Chimie Bio Organique et Macromoléculaire,*
Departement of Chemistry, University Cadi Ayyad Marrakech, Marrakech, Morocco
[c]*École Supérieur de Technologie, University Ibn Zohr Laayoune, Laayoune, Morocco*
**e-mail: adlounisou@gmail.com*

Received November 11, 2016
Revised January 17, 2018
Accepted February 28, 2019

Abstract—The interaction between Cr(III) and "chitosan/montmorillonite" nanocomposites has been studied. Also, the adsorption kinetic of chromium in prepared chromium solution and in tannery wastewater has been presented. The article confirmed the initial interest in using "chitosan/montmorillonite" nanocomposites as depolluting agent, especially MMTCTf2% nanocomposite exhibits the best adsorption capacity of Cr(III) as compared to MMTCTf1% and MMTCTf3%. According to ICP-OES analysis MMCTf2% can adsorb 45% of Cr(III) from this effluent.

DOI: 10.3103/S1063455X1903007X

Keywords: chitosan, montmorillonite, nanocomposite, chromium complexation, wastewater.

INTRODUCTION

Chitosan and clay exhibit a good adsorption capacity of metallic ions [1]. The free amine function gives to chitosan a better ability to chelate metallic ions [2].

Recently, polymer-clay nanocomposites have received significant attention because nanocomposites present an excellent nano-scale dispersion, which brings significant improvement in mechanical and physical properties as compared to micro-scale polymer composites. Different studies confirm the enhance of mechanical properties [3], thermal stability [4, 5], functional properties [6], barrier properties [6, 7] and water solubility [7] of chitosan nanocomposites by incorporation of nanoclay (1–5 wt %) into chitosan.

Montmorillonite is the most widely studied type of clay; it has an important atoms substitutions and disorganized piling of sheets. This disorder and the decreasing load of sheets increase the interlamellar space, which allows an easier adsorption of water, cations and organic molecules [8].

The modification of montmorillonite by chitosan improves its adsorption capacity. Hence, chitosan is introduced into interlamellar space of montmorillonite, obtaining "chitosan-montmorillonite" nanocomposites. These nanocomposites are prepared using acetic acid or ascorbic acid, the obtained suspension of montmorillonite was added to chitosan solution. Therefore, the properties of surface and particle size of nanocomposites are better using acetic acid [9].

The present study was aimed to determine the best "chitosan/montmorillonite" nanocomposites for complexing of chromium ions present in tannery wastewater. First, using Infrared spectrum and contact angle, we established the presence of interaction between Cr(III) and nanocomposites. Then, the adsorption kinetic of Cr(III) revealed that chitosan reinforced by 2% of montmorillonite MMTCTf2% is the best complexing nanocomposite. Therefore, the obtained results encouraged us to use our nanocomposites MMTCTf1%, MMTCTf2% and MMTCTf3%, to eliminate chromium ions from a real effluent, recuperated from tannery wastewater of Marrakech in Morocco. Finally, according to ICP-OES and UV-Vis analysis we have shown that MMCTf2% nanocomposite are still present the best adsorption capacity in effluent as well.

---

[1] The text was submitted by the authors in English.

EXPERIMENTAL

Montmorillonite used for preparation of nanocomposites were obtained from "Sigma-Aldrich". Chitosan with average molecular weight of 63 kDa and 96% deacetylation degree was prepared according to our previous study [10]. Chromium ions were used as chlorides form $CrCl_3$ obtained from "Sigma-Aldrich", this form was preferred due to the fact that sulfate salts are mostly insoluble and nitrates may act as oxidants; moreover, they adsorb in ultraviolet region, which may complicate the obtaining and interpretation of our results.

Preparation of "Chitosan/Montmorillonite" Nanocomposites

Nanocomposites were prepared according to the study [11]. First, selected amounts of montmorillonite (1; 2 and 3% on solid chitosan) were dispersed in 100 mL of 1% (*v*/*v*) aqueous acetic acid solution and intensively stirred for 24 h. Then, chitosan solution was prepared by dissolving 20 g of chitosan powder in 100 mL of aqueous acetic acid solution 1% (*v*/*v*), under intensive stirring at 90C for 20 min and cooled at room temperature. Afterward, 150 mL of chitosan solution was added to the clay solutions and stirred for 4 h. The blends were dropped into a Teflon dish and let to dry. Once nanocomposites formed, they were removed from dishes and conditioned in a desiccator at 57% relative humidity, using saturated solution of sodium bromide at ambient temperature.

The formed nanocomposites (MMTCTf1%, MMTCTf2% and MMTCTf3%) were in the NH_3^+ form, they were dipped in a 0.4 M sodium hydroxide solution to reach the uncharged amino form. After 5 min, we washed the prepared chitosan-based sorbent (MMTCTf1%, MMTCTf2% and MMTCTf3%) with water to eliminate salts. After drying, our nanocomposites are insoluble in water and ready for sorption study [12].

Fourier Transform Infrared (FTIR) Spectroscopy Analysis

FTIR spectra were recorded on a Fourier transform infrared spectrometer Bruker VERTEX-70 using vacuum for reference. Spectra were collected in the 4000–400 cm^{-1} range with 32 scans at 4 cm^{-1} resolution.

Scanning Electron Microscopy Analysis

The morphology of "chitosan/montmorillonite" nanocomposites was observed using scanning electron microscopy. Samples were coated with graphite under vacuum using an automatic sputter coater. The analyses were conducted using a scanning electron microscope Quanta 200 operating at an accelerated voltage of 20 kV for all of films.

Contact Angle

Surface hydrophobicity of films was estimated by sessile drop method, based on optical contact angle method. Contact angle measurements were carried out with a drop shape analysis (DSA1) from "Krüss". A droplet of solvent was deposited on films surface with an automatic piston syringe. The drop image was photographed using a digital camera. An image analyzer was used to measure angle formed between the surface of film in contact with the drop and tangent of liquid drop at the point of contact with film surface. Measurements were performed within the first 15 s after dropping the solvent onto film surface, to avoid variations due to solvent penetration onto the specimens. Many measurements were performed for each film at room temperature with ethylene glycol, glycerol and water as droplet solvent.

UV-Vis Analysis

A Specord 210 plus spectrophotometer UV-Vis from "Analytik Jena", covering the wavelength range from 200 to 800 nm, with quartz cells with a thickness of 0.2 cm; allowed us to identify two characteristic bands of Cr(III) at 430 and 617 nm. Also, using the calibration curve we determined chromium concentration remained in solution after sorption process, in order to calculate the adsorbed quantity of Cr(III) and adsorption capacity of nanocomposites.

ICP-OES Elemental Analysis

A Perkin Elmer Optima 2000 Inductively Coupled Plasma-Optical Emission Spectrometer (ICP-OES), was used to determine the quantity of chromium persistent in tannery wastewater after complexation phenomenon. Standard solutions for instrument's calibration curve were prepared as follows: 10 mL of 1000 mg/L of

ICP standard diluted to 100 mL with DI water which served as stock solution. Subsequently, different volumes of the stock solution (0.05; 0.1; 0.5; 1.0; 2.0; 4.0; 6.0 and 10.0 mL) were pipetted into 100 mL volumetric flasks and diluted to mark.

RESULTS AND DISCUSSION

Characterization of "Chitosan/Montmorillonite" Nanocomposites

Nanocomposites MMTCTf1%, MMTCTf2% and MMTCTf3% exhibit in infrared spectrum (Fig. 1) characteristic peaks between 3500 and 3000 cm^{-1}, attributed to stretching vibration of free hydroxyl and to asymmetric and symmetric stretching of N–H [13]. Also, the spectrum shows characteristic stretching and bending vibration of the adsorbed water H–O–H at 3425 and 1540 cm^{-1}, and also at 1430 cm^{-1} characteristic –OH plane bending [14].

Moreover, a characteristic peak at 1020 cm^{-1} can be attributed to Si–O stretching vibration, which could reveal the existence of hydrogen-bonding sites for functional groups of chitosan [15]. These peaks are stronger for MMTCTf2% nanocomposite; this could be attributed to hydrogen bonding between –OH group in MMT and functional groups –NH and –OH in chitosan. There exist also characteristic vibrations of Si–O–Al at 570 cm^{-1}.

The scanning electron microscopic images of prepared sorbent chitosan/montmorillonite nanocomposites (Fig. 2) present smooth, homogeneous surfaces without pores. The phenomenon can be attributed to the dispersion of montmorillonite (1; 2 and 3%) particles in to chitosan matrix, these results are similar to those reported in [7]. This interaction becomes more obvious for the reinforcement of chitosan by 2%. Also, some small irregularities for MMTCTf1% and MMTCTf3% nanocomposites were observed.

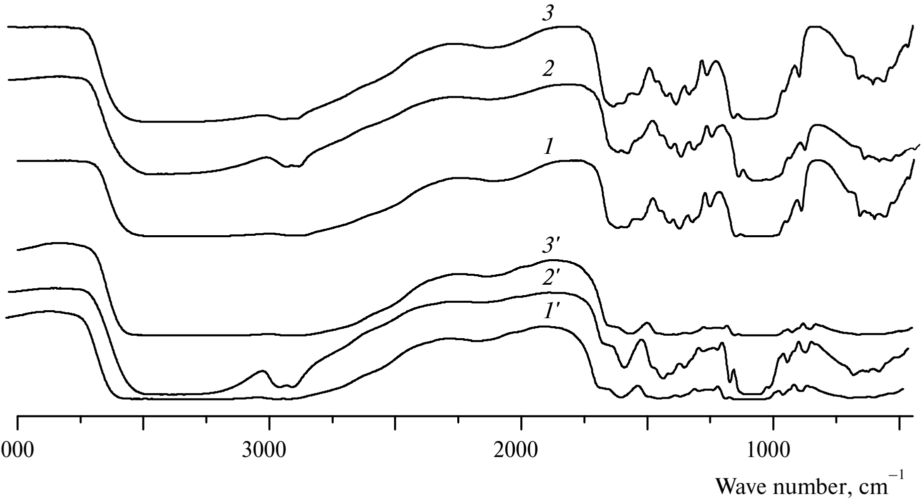

Fig. 1. Infrared spectrum of nanocomposites "chitosan/montmorillonite" before MMTCTf1% (*1*), MMTCTf2% (*2*), MMTCTf3% (*3*) and after adsorption of MMTCTf1%-Cr (*1'*), MMTCTf2%-Cr (*2'*) and MMTCTf3%-Cr (*3'*).

Contact angle method is a simple way to determine the excessive hydrophilicity of films, because using water or another polar solvent contact angle will increase with increasing surface hydrophobicity [16–18]. Polarity of surface and its tension were calculated using the model [19]:

$$\Upsilon_L(1-\cos\theta) = 2\sqrt{\Upsilon_L^d\Upsilon_S^d} + 2\sqrt{\Upsilon_L^p\Upsilon_S^p},$$

where θ stands for contact angle between solid film and liquid drop; Υ_L is surface tension of liquids (water, ethylene glycol and glycerol); Υ^d and Υ^p are the dispersive and polar components of surface tension of solid (S) and liquid (L).

According to the results of the table, the dispersive and polar components are close for MMTCTf1% nanocomposite. However for MMTCTf2% and MMCTf3% nanocomposites, we note that the polar component increases when the reinforcement of chitosan by montmorillonite increases. It can be explained by the polarity of montmorillonite which can be dispersed easily into chitosan. As a result, we conclude that the surface tension is more important for MMTCTf3%.

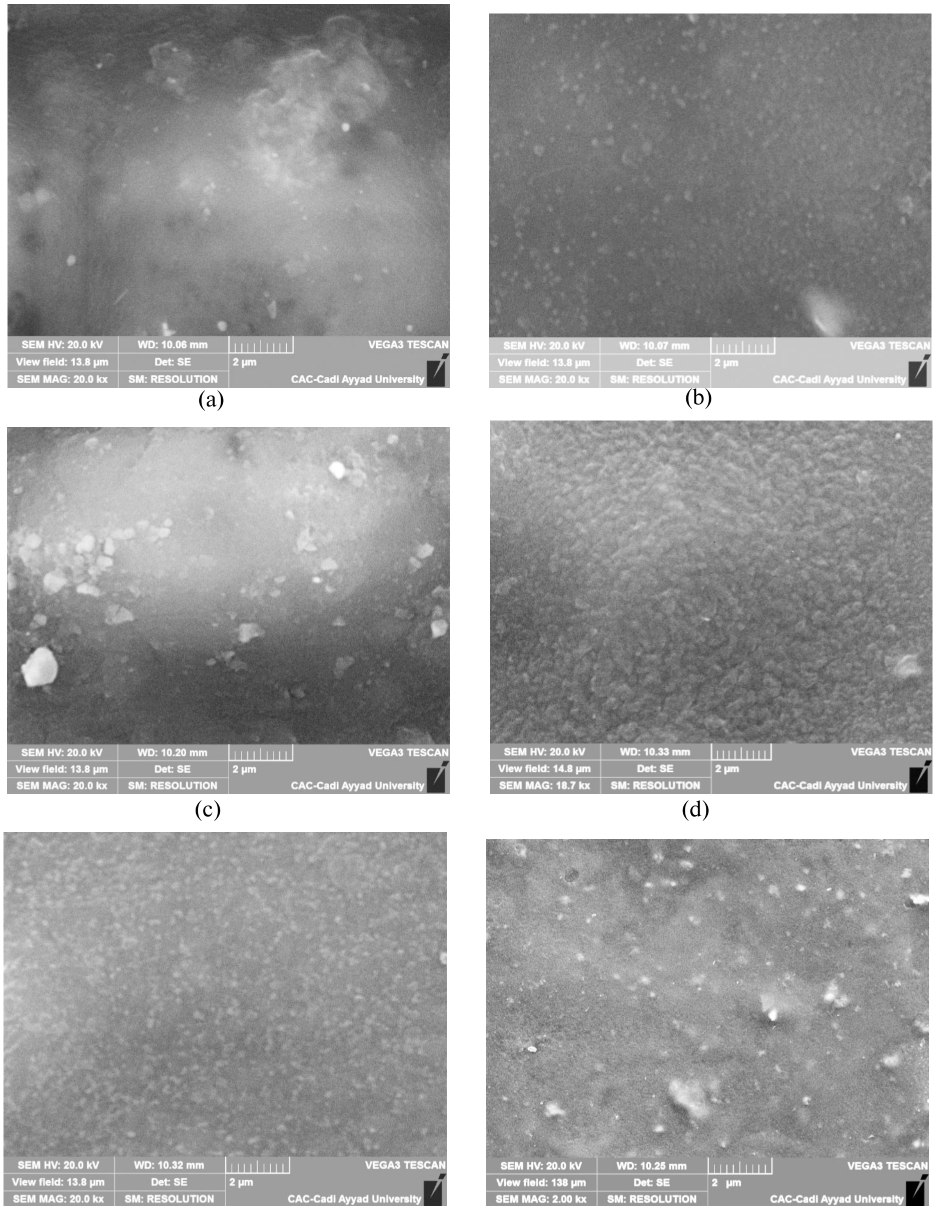

(a) (b)

(c) (d)

(e) (f)

Fig. 2. Scanning electron microscopy of our nanocomposites before MMTCTf1%, MMTCTf2% and MMTCTf3% (a–c) and after adsorption of Cr(III) MMTCTf1%–Cr, MMTCTf2%–Cr and MMTCTf3%–Cr (d–f) in chromium solution.

Adsorption Kinetic of Cr(III)

We located the adsorption band of Cr(III) at 430 nm, the concentration of chromium solution was 250 mg/L, its pH was 6.6. Also the mass of MMTCTf1%, MMTCTf2% and MMTCTf3% nanocomposites were fixed at 2 mg, afterwards we added nanocomposites to 10 mL of chromium solution, then we monitored the adsorption quantity of Cr(III) using UV-Vis analysis every 10 min. Subsequently, the concentration of persistent Cr(III) was determined using the calibration curve of UV-Vis analysis. After that we calculated the adsorbed quantity of Cr(III) during 70 min (Fig. 3a) according to the equation

$$Q_{\text{ads}} = (C_i - C_r) \times 100/C_i, \tag{1}$$

where Q_{ads} is adsorbed quantity of Cr(III), %; C_i is the initial concentration of chromium in solution, mmol/L; C_r is chromium concentration remained in solution, mmol/L.

Characterization data of contact angle and surface tension of nanocomposites before MMTCTf1%, MMTCTf2% and MMTCTf3% and after adsorption of Cr(III) MMTCTf1%–Cr(III), MMTCTf2%–Cr(III) and MMTCTf3%–Cr(III)

Nanocomposite	Contact angle, deg			Υ_{Sd}	Υ_{Sp}	Υ_{total}
	θ_W	θ_{EG}	θ_{GL}			
Natural film						
MMTCTf1%	67.1	49.8	50.8	18.3	19.01	37.31
MMTCTf2%	65.5	49.5	58.5	11.22	26.37	37.59
MMTCTf3%	40.3	32.4	60.5	0.4	77.35	77.75
Film–Cr(III)						
MMTCTf1%	89.8	66.4	80.8	16.20	6.88	23.08
MMTCTf2%	80.5	59.7	56.5	28.49	6.32	34.81
MMTCTf3%	80.5	53.7	39.5	50.79	1.74	52.53

Note. Υ_{Sd}—dispersion forces; Υ_{Sp}—polar forces; Υ_{total}—surface tension; W—water; EG—ethylene glycol; GL—glycerol.

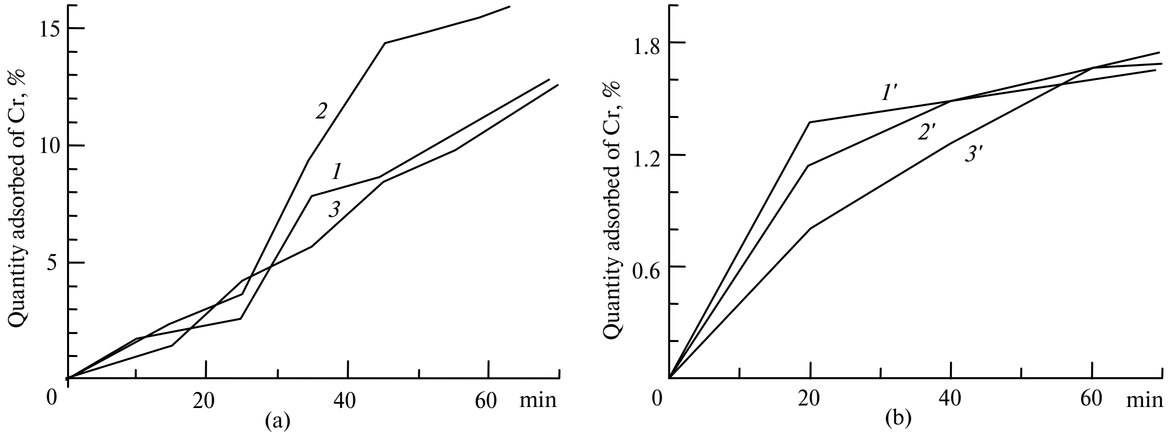

(a) (b)

Fig. 3. Adsorbed quantity of Cr(III) in solution of $CrCl_3$ (a) and in tannery wastewater (b) by MMTCTf1% (*1, 1'*), MMTCTf2% (*2, 2'*) and MMTCTf3% (*3, 3'*) nanocomposites.

The curves of adsorption kinetic (see Fig. 3a) reveal that during 15 min of contact, adsorbed quantity of MMTCTf1% and MMTCTf2% nanocomposites is similar, approximately 2% of Cr(III) was adsorbed after 20 min. This quantity is increasing with time; MMTCTf2% adsorbs 15%, MMTCTf1% 12% and MMCTf3% 9% after 70 min of contact. We estimate that the best complexing nanocomposite of Cr(III) is MMCTf2%. Therefore, from these results we conclude that the adsorption capacity of nanoccomposites can be improved by increasing the mass of the sorbent.

Adsorption Capacity of Nanocomposites

In prepared chromium solution (250 mg/L), we determined the capacity of nanocomposites to complex Cr(III) after 70 min of interaction. The adsorbed capacity was calculated according to the following equation:

$$CP_{ads} = \frac{(C_i - C_r) \cdot V}{M}, \tag{2}$$

where CP_{ads} is adsorbed capacity of chromium, mg/g; C_i is the initial concentration of $CrCl_3$ solution, mg/L; C_r is the chromium concentration remained in solution, mg/L after 70 min of contact, determined using the calibration curve of UV-Vis analysis; M is the mass of nanocomposites, g; V is the volume of chromium solution, L.

The results of Fig. 4 confirm that the best complexing nanocomposite is MMCTf2%. We conclude that for best adsorption of Cr(III) by our sorbent, the critical reinforcement of chitosan by montmorillonite is 2%

(MMTCTf2%), beyond this ratio the adsorption capacity becomes the same as that for the reinforcement by 1% (MMTCTf1%) and this is the case of MMTCTf3% nanocomposite.

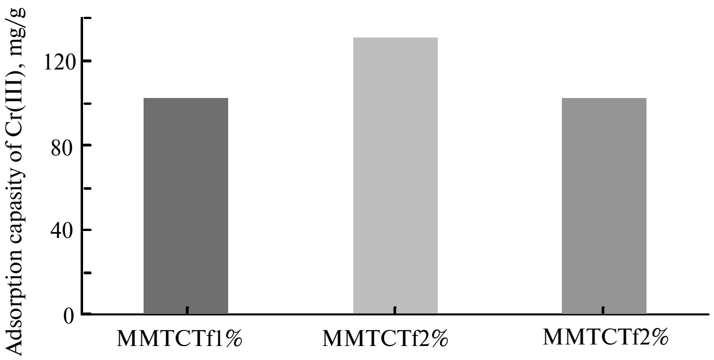

Fig. 4. Adsorption capacity of Cr(III) ions by MMTCTf1%, MMTCTf2% and MMTCTf3% after 70 min of contact.

Interaction "Nanocomposites–Chromium (III)"

Samples were recovered after 70 min of contact and let to dry before characterization.

The infrared spectrum (see Fig. 1) shows that the peak of –OH bending vibrations at 1430 cm^{-1}, shifted to 1330 cm^{-1} after adsorption of Cr(III) for the three nanocomposites. However, this peak is more intense and narrow. Also, we observed a weak peak which emerged around 1400 cm^{-1}. These results confirm the interaction between Cr(III) ions and prepared nanocomposites.

After adsorption of Cr(III) the three nanocomposites become light green and rigid. According to SEM images (see Fig. 2) the morphologies of MMTCTf1% changed, its surface is cloud-like (MMTCTf1%–Cr). This can be explained by the sorption of Cr(III) by MMTCTf1% nanocomposites. Besides, Fig. 2 reveals the presence of small white spots for MMTCTf2%–Cr; they are lesser and dispersed for MMTCTf3%–Cr. This phenomenon can be attributed to the interfacial interaction between our sorbent and chromium ions.

In addition we studied the contact angle after adsorption of Cr(III). The obtained results shown in the table reveal that dispersive components of surface tension of MMTCTf2% and MMCTf3% nanocomposites increase, with decreasing of polar component of MMTCTf1%. This change of surface tension indicate that the hydrophilicity of nanocomposites decreases after adsorption of Cr(III). It can be explained by the interfacial interaction between Cr(III) and MMCTf1%, MMCTf2% and MMCTf3% nanocomposites.

Chromium Adsorption in Tannery Wastewater

Tanneries localized in Old Medina Marrakech-Morocco contain an important tannery waste which is disposed of without treatment. On one hand, this waste could be used in agiculture, because they contain phosphor and nitrogen. On the other hand, heavy metals (Cd, Cu, Ni, Cr etc.) present in the tannery waste can contaminate vegetable and subsequently disturb the food chain [20]. To avoid this problem of toxicity by metallic ions, we are interested in the elimination of chromium from tannery wastewater. The pH of recuperated tannery wastewater was 6, its concentration in Cr(III) was 300 mg/L determined via the calibration curve by UV-Vis analysis.

To study the adsorption kinetic of chromium in tannery wastewater, we used the same procedure as explained above. First, we fixed the adsorption band of Cr(III) at 430 nm, then we added MMTCTf1%, MMTCTf2% and MMTCTf3% nanocomposites to tannery wastewater. Subsequently, the concentration of persistent Cr(III) was determined using the calibration curve of UV-Vis analyses. After that the adsorbed quantity of Cr(III) ions was calculated according to Eq. (1).

Results of Fig. 3b reveal that during 60 min, the adsorbed quantity of Cr(III) increases for the three nanocomposites. After 60 min the changes appear which can be explained by the saturation of MMTCTf1%, MMTCTf2% and MMTCTf3% nanocomposites. Thus, the results confirm that the sequence of the best complexing nanocomposites in tannery wastewater is in consistency with the sequence in chromium solution. However, the adsorbed quantity is more significant in chromium solution. This can be explained by presence of competition between chromium and other metallic ions in tannery wastewater (Cd, Cu, Ni etc.).

To confirm these results we determine the persistent quantity of Cr(III) in effluent using ICP-OES analysis. We added 2 mg of nanocomposites to 10 mL of tannery wastewater, after 24 h of interaction we analyzed the effluent by ICP-OES spectroscopy. Then we illustrate the remained quantity of chromium after adsorption process by each nanocomposite (Fig. 5).

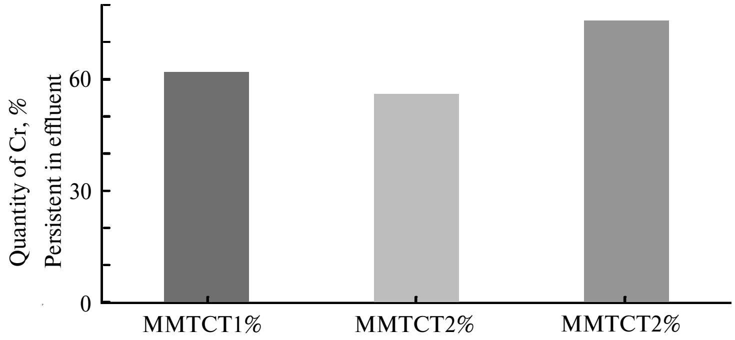

Fig. 5. Quantity of Cr(III) remained in tannery wastewater after adsorption process by MMTCTf1%, MMTCTf2% and MMTCTf3% nanocomposites.

Figure 5 shows that MMTCTf2% still presents the best adsorption capacity, after 24 h of contact with tannery wastewater MMCTf2% can adsorb 45% of Cr(III). This confirms the obtained results of kinetic study in tannery wastewater and chromium solution as well. In these conditions we can deduce the following sequence, of the best complexing nanocomposite of Cr(III): MMCTf2% > MMCTf1% > MMTCTf3%.

CONCLUSIONS

We prepared and characterized our sorbent by reinforcing chitosan with different ratio of montmorillonite. The obtained nanocomposites MMTCTf1%, MMCTf2% and MMTCTf3% present a good adsorption capacity of Cr(III). Moreover, MMTCTf2% nanocomposite is the best sorbent in chromium solution and in tannery wastewater as well. Also, according to ICP-OES analysis, MMTCTf2% adsorbs 45% of Cr(III) after 24 h of interaction in tannery wastewater. Nevertheless, due to the presence of other metallic ions in tannery wastewater, the adsorbed quantity is lower than that of chromium solution.

REFERENCES

1. Crini, G., *Progress in Polymer Sci.,* 2005,vol. 30, pp. 38–70.
2. Sashiva, H., Aiba, S., *Progress in Polymer Sci.,* 2004, vol. 29, pp. 887–908.
3. Lavorna, M., Piscitelli, F.,Maniacapra, P., and Buonocore, G.G., *Carbohydrates Polymers,* 2010, vol. 82, no. 2, pp. 291–298.
4. Darder, M., Colilla, M., and Hitzky, E.R., *Chem. of Materials,* 2003, vol. 15, no. 20, pp. 3774–3780.
5. Wang, S., Shen, L., Tong, Y., et al., *Polymer Degradation and Stability,* 2005, vol. 90, pp. 123–131.
6. Rhim, J., Hong, S., Park, H., and Hg, P., *J. Agricult. And Food Chem,* 2006, vol. 54, no. 1, pp. 5814–5822.
7. Casariego, A., Souza, B.W.S., Cerqueira, M.A., et al., *Food Hydrocol.,* 2009, vol. 23, no. 7, pp. 1895–1902.
8. Azeredo, H., *Food Res. Int.,* 2009, vol. 42, no. 9, pp. 1240–1253.
9. Darder, M., Colilla, M., and Hitzky, E.R., *Appl. Clay Sci.,* 2005, vol. 28, pp. 199–208.
10. Dahmane. E.L., Taourte,M., Eladlani, N., and Rhazi, M., *Int. J. Polymer Anal. Charact,* 2014, vol. 19, pp. 1–10.
11. Xu, Y., Ren, X, and Hanna, M., *J. Appl. Polymer Sci.* 2006, vol. 99, no. 4, pp. 1684–1691.
12. Rhazi, M., Desbieres, J., Tolaimate, A., et al., *Eur. Polym. J.,* 2002, vol. 38, pp. 1523–1530.
13. Siripatrawan, U. and Harte, B.R., *Food Hydrocol.,* 2010, vol. 24, no. 8, pp. 770–775.
14. Wang, X, Du, Y., and Luo, J., *Nanotechnol.,* vol. 19, no. 6, p. 065707.
15. Tunc, S. and Duman, O., *Colloids and Surfaces, A.,* 2008, vol. 317, pp. 93–99.
16. Hambleton, A., Fabra, M.J., *Debeaufort, F., et al., J. Food Eng.*, 2009, vol. 93, pp. 80–88.
17. Pereda, M. and Aranguren. M.I., *Food Hydrocol.,* 2010, vol. 24, pp. 800–808.
18. Zia, K.M., Zuber, M., Mahboob, S., et al., *Carbohydrate Polym.,* 2010, vol. 80, pp. 229–234.
19. Owens, D.K. and Wengt, R.C., *J. Appl. Polymer. Sci.,* 1961, vol. 13, pp. 1741–1747.
20. Vatribi, A., Nejmeddine, A., and Boukhars, L., *Sud. Sci. and Technol.,* 2000, no. 6, pp. 27–34.